Trees (2026) 40:20
https://doi.org/10.1007/s00468-026-02727-0

ORIGINAL ARTICLE

Evaluation of the box-counting method for assessing tree structures: A case study of European beech (*Fagus sylvatica* L.)

Tatsuro Kikuchi[1] · **Konstantin Köthe**[1] · **Alice Penanhoat**[1,3] · **Dominik Seidel**[1,2]

Received: 12 July 2025 / Accepted: 15 January 2026

Key message

The box-counting method is sensitive to tree positions in the coordinate system, and based on this method, assuming self-similarity of beech tree models derived from mobile laser scanning was difficult.

Abstract

The repetitive branching architectures of trees lead us to think that trees exhibit self-similarity and fractal properties. Therefore, applying fractal analysis to assess tree structures may seem natural. This study aimed to evaluate the box-counting method (BCM), a simple and commonly used fractal analysis, for describing 3D biological trees, using a wide range of structural models of European beech trees (*Fagus sylvatica* L.) derived from mobile laser scanning. We specifically investigated the method's sensitivity to the arbitrary placement of a tree within the coordinate system and the validity of the tree's self-similarity based on the BCM. The BCM was sensitive to the tree position in the coordinate system, with observed minimum and maximum variations in the box-counting dimension (D_b) values of 0.18 and 0.52, respectively, when translating the trees in the XYZ directions. The analysis of the local slopes of the BCM, which are the slopes between neighboring data point pairs, revealed a large variation of slope values across scales with a clear pattern, indicating that the structural patterns of the sampled trees were inconsistent and locally dependent. Thus, it is difficult to assume self-similarity of the beech tree models based on the BCM. Our results demonstrate the need to standardize the computation of the D_b for single trees with respect to the coordinate system and caution in interpreting the D_b. These findings contribute to a deeper understanding of the D_b to assess tree structures and functions.

Keywords LiDAR · Box-dimension · Fractal analysis · Tree architecture · Sensitivity · Self-similarity

Introduction

Approximately 73,000 tree species are estimated to exist globally (Cazzolla Gatti et al. 2022). Thus, we can naturally expect a large aboveground structural diversity between species. At the same time, there are large structural differences within species due to ontogenetic variation, phenotypic plasticity, and genetic variation (Laurans et al. 2024). Therefore, the observation of tree branching and growth patterns tends to suggest different architectural models of trees; however, it also suggests a tendency to reiteration of architectural units as a general characteristic (Barthélémy and Caraglio 2007). The reiteration may indicate that trees can be considered as self-similar and fractal objects (Malhi et al. 2018). Thus, the application of fractal analysis was anticipated to facilitate the analysis of complex tree-branching architectures. The recent advancement of remote

Communicated by H. Roaki Ishii

✉ Tatsuro Kikuchi
tatsuro.kikuchi@stud.uni-goettingen.de

[1] Department of Spatial Structures and Digitization of Forests, University of Göttingen, Büsgenweg 1, 37077 Göttingen, Germany

[2] Centre of Biodiversity and Sustainable Land Use (CBL), University of Göttingen, Büsgenweg 1, 37077 Göttingen, Germany

[3] Division of Forest Remote Sensing, Swedish University of Agricultural Sciences, Skogsmarksgränd 17, 907 36 Umeå, Sweden

Published online: 30 January 2026

sensing technologies, especially ground-based laser measurements (i.e., terrestrial and mobile laser scanning), facilitated and increased the accuracy of capturing the detailed three-dimensional (3D) structures of natural trees (Malhi et al. 2018; Dorji et al. 2021), which opened up the potential for applying fractal analysis. Among the many available fractal analyses, the box-counting method (BCM) has been commonly used due to its straightforward calculation procedure for measuring tree structural complexity (e.g., Seidel 2018; Guzmán et al. 2020).

What is the BCM?

The BCM counts the number of grids or boxes in a grid system that intersect the object of interest with varying box edge lengths. When the object tends to be self-similar, which means when magnified, the magnified portion resembles the whole, the relationship between the number of boxes and the inverse of the box edge length approximately follows a power law. This is because the amount of detail that appears at different scales is constant for a self-similar object (Falconer 2003, 2013). In such a case, taking the logarithm of both the number of boxes and the inverse of the box edge length and doing a linear regression gives us a straight line. The slope of the regression line (i.e., the scaling exponent of the power law) is the box-counting dimension (D_b) and the estimated fractal dimension of the object (Bouda et al. 2016). Thus, the D_b can also be interpreted as the constant logarithmic rate of the increase of the box number with respect to the logarithmic decrease of scale. The R^2 value from the linear regression is often used to assess the consistency of the scaling properties (i.e., self-similarity) of the object.

The D_b is equal to one when the object is a perfect pole (one dimension) because when the box size halves, the number of boxes becomes two to the power of "one," and the D_b is three when the object is a homogeneously filled cube because when the box size halves, the number of boxes becomes two to the power of "three." Tree growth leads to filling up of the 3D space, but the amount of volume occupied is modulated by competition and self-shading, resulting in individual trees having a D_b value between 1 and 3 (Seidel 2018). In an applied sense, D_b is considered the structural complexity index that simultaneously accounts for the density and distribution of the object's elements and has been used as a space-filling character (Seidel 2018).

What does the D_b tell us about the tree structure?

Trees are complex, ramified objects, and describing their structure is complicated. In particular, the branching pattern is difficult to characterize because using single measurements, such as mean branch diameter, mean branch angle, or mean number of branches, reduces information about the spatial distribution of these elements (Seidel 2018). Moreover, differences in branching patterns, including the degree of ramification and branching order, can complicate comparisons across trees. Thus, although the D_b is linked to structural metrics such as the mean crown radius, crown surface area (the convex hull of the tree crown) or branch angles (Seidel et al. 2019b), it captures more information about their distribution in space, which is an essential feature that determines and indicates the biological functions of the tree, including its capacity to intercept light.

Correlative studies between the D_b and tree functioning found positive relationships with productivity (Seidel 2018; Seidel et al. 2019a; Dorji et al. 2021), positive relationships with branch hydraulic efficiency, and negative relationships with hydraulic safety (Dorji et al. 2024). Moreover, in a deciduous forest, vital trees tended to show a larger difference in D_b between summer and winter than less vital trees, due to the differences in foliage development (Heidenreich and Seidel 2022). These accumulating results suggest that the D_b can be a helpful index in tree structure-function research.

Potential issues of the D_b

Although the BCM can be easily applied, the D_b value can be sensitive to the arbitrary placement of an object in the 3D grid system. This is because the number of boxes intersecting the object at each scale depends on the object's position and orientation within the grid system (Da Silva et al. 2006; Bouda et al. 2016). Currently, the BCM is often applied to the point clouds of trees obtained from terrestrial or mobile laser scanning (e.g., Saarinen et al. 2021; Dorji et al. 2021, 2024), and the box-counting procedure is likely done based on the coordinates of the point clouds, which depend on how the laser scanning was conducted. Therefore, even if we have ideal occlusion-free point clouds, applying the BCM to the tree point clouds may produce the D_b specific to the tree's position and orientation in the coordinate system. In this study, we define the placement effect as the sensitivity of D_b to tree positions and orientations in the coordinate system. In literature, a similar but different term, quantization error, is used to describe the deviation between the empirical and the minimum box counts required to cover the object (Bouda et al. 2016). A large placement effect may potentially decrease the association between the D_b and the tree's physical functions (Loke and Chisholm 2022). However, the placement effect is usually neglected in the literature. Thus, characterizing the placement effect is crucial for the further application of the D_b to reliably describe natural tree structures.

It is expected that trees with higher architectural self-similarity with repeated branching produce higher R^2 values of the regression lines than those with less architectural self-similarity (Seidel 2018), as R^2 values are supposed to measure the consistency of a scaling exponent or the degree of self-similarity. For 3D trees based on point clouds, R^2 values are usually very high (>0.96) (e.g., Guzmán et al. 2020), and we might be tempted to conclude that trees are indeed self-similar. However, a high R^2 value may not be a sufficient measure of self-similarity, as the data points used in the linear regression are correlated and violate the statistical assumption of independence, leading to inflated R^2 values (Reeve 1992). To determine how much a tree's structural scaling pattern may actually change across different scales, we can additionally compare local slopes, which are the slopes between neighboring data point pairs. If a tree is approximately self-similar within the interested scales, we expect local slope values to be reasonably stable across scales (Halley et al. 2004; Bouda et al. 2016). Some studies demonstrate that local slopes vary across scales with a clear pattern when objects' structural patterns depend on specific scales (Panico and Sterling 1995; Bouda et al. 2016; Cheeseman and Vrscay 2022). To improve the interpretation of the D_b, it is important to examine R^2 values as well as local slope patterns under different levels of branch reiteration. If trees are approximately self-similar, reducing the branching repetition should disrupt their self-similarity, which will be reflected in R^2 values and local slope patterns.

The present study aimed to investigate (1) the BCM's sensitivity to arbitrary tree placement in the coordinate system, and (2) R^2 values and local slope patterns of the BCM under different levels of branch reiteration.

Methods

We used 100 Quantitative Structure Models (QSMs) of European beech (*Fagus sylvatica* L.) as reference tree objects. We chose European beech because it is a productive and ecologically important species that dominates a wide range of European forests and provides valuable wood for many purposes (Durrant et al. 2016). Thus, efficiently quantifying their structural complexity would help forest management. We used QSMs because they can be used to create (1) occlusion-free point clouds by converting the QSMs to point clouds and (2) different levels of branch reiteration by artificially pruning the trees using the QSM branch order information.

Study site

The present study was conducted on two 50 m x 50 m plots of pure European beech stands located in Nienover and Unterluess, Lower Saxony, Germany. The Nienover plot in southern Lower Saxony is at 320 m.a.s.l., while the Unterluess plot lies further north at 162 m.a.s.l. Both sites share a temperate climate with similar mean annual air temperatures of 8.8 °C and 9.0 °C, while mean annual precipitation is slightly higher in Nienover (895 mm) compared to Unterluess (747 mm). The stands are approximately 85 years old and have been managed until 2018. Although trees of the genera *Picea*, *Larix*, *Quercus*, *Pseudotsuga*, and *Pinus* were present, European beech was the main stock for both plots, accounting for at least 70% of the trees.

Mobile laser scanning and point cloud processing

In March 2021, both plots were scanned during leafless conditions using a mobile laser scanner (ZEB-Horizon, Geoslam Ltd., Nottingham, UK). Utilizing a 903 nm laser, the device emits 300,000 points per second, reaching a maximum distance of 100 m and detecting the traversed environment with a 3 cm range of noise. Point clouds and the respective trajectories were generated using the Simultaneous Localization and Mapping (SLAM) algorithm in GeoSLAM Hub 6.0 (GeoSLAM Ltd., Nottingham, UK). Individual tree segmentation was achieved using LiDAR360 (GreenValley International Ltd., California, USA). The preceding density homogenization to a 0.5 cm resolution, manual correction, and final noise filtering were carried out in CloudCompare (version 2.13.0; https://www.danielgm.net/cc/). The respec tive noise filtering function was set to a sphere radius of 0.2 m and a relative maximum error of 1.0.

QSMs

QSMs were obtained using the SimpleTree plugin (Hackenberg et al. 2015) in CompuTree 5.0 (Piboule et al. 2013). QSMs reconstruct a tree's branching structure using hierarchically fitted cylinders, which are set by a non-linear least squares fitting routine around a tree point cloud (Hackenberg et al. 2014, 2015). Since the whole branching architecture was of interest, all cylinders up to the highest available order of each tree were included. Upon visual inspection, the 100 best-fitting QSMs were chosen for further analysis.

Pruning

First, we improved the QSMs using the Real Twig method (Morales and MacFarlane 2024), which corrected the overestimation of small branch and twig cylinder sizes based

on the species-specific twig diameter information using the function *run_rtwig* from the R package *rTwig* (Morales and MacFarlane 2024). Then, we removed specific orders of branches (4th or more, 3rd, and 2nd orders; 0th order is the main stem) sequentially from the QSMs in R version 4.4.2 (R Core Team 2024) (Fig. 1), resulting in 399 QSMs (one tree has the maximum branch order of three), including without pruning. Thereafter, the QSMs were exported as mesh files using the function *export_mesh* from the R package *rTwig*. Then, using the command-line mode of CloudCompare (version 2.14.alpha; https://www.danielgm.net/cc/), we simulated point clouds with a precision of 1 cm and a density of 5000 points per m^2 based on the mesh files for the following D_b computation. Lastly, in R, we updated the coordinate origin (0, 0, 0) to the point's coordinate with the lowest Z coordinate of a tree (i.e., the tree base) and considered the tree's position and orientation as the reference. When there were multiple points with the lowest Z coordinate, we averaged the X and Y coordinates of those points. This standardization of tree position within the coordinate system was necessary for the following processes related to the placement effect.

Computing D_b

Using the function *box_dimension* from the R package *rTwig* (Morales and MacFarlane 2024), we computed the D_b. The codes are written based on previous studies investigating the D_b in tree structural complexity (Seidel 2018; Seidel et al. 2019a; Arseniou et al. 2021a). First, the largest edge length of the box (more precisely, voxel) was determined as the maximum of the ranges of the X, Y, and Z coordinates in the point clouds. Then, the largest edge length was subsequently halved until it reached the lower cutoff point (Fig. 2A). A box size with each edge length was used for the following box-counting process. We set the lower cutoff to 20 cm as a conservative estimate of the minimum point-cloud resolution in our mobile laser-scanning data.

Voxelization was done to count the number of boxes of each edge length. First, the original point coordinates (in m) were scaled by the respective box edge lengths, and then the scaled coordinates were floored to assign the points to the boxes to which they belong. Lastly, the number of unique coordinates was counted as the number of boxes. To compute the D_b, ordinary least squares regressions were used with log(N) being the response and log(1/r) being the predictor (log: natural logarithm; N: the number of boxes; r: relative box edge length with respect to the largest box edge length) (Fig. 2B). We removed the data point related to the initial box from the D_b computation since including the largest box size is expected to increase the placement effect due to the small box counts (Panico and Sterling 1995; Loke and Chisholm 2022), setting the argument *rm_int_box = TRUE* in the function *box_dimension*. R^2 values from the regression

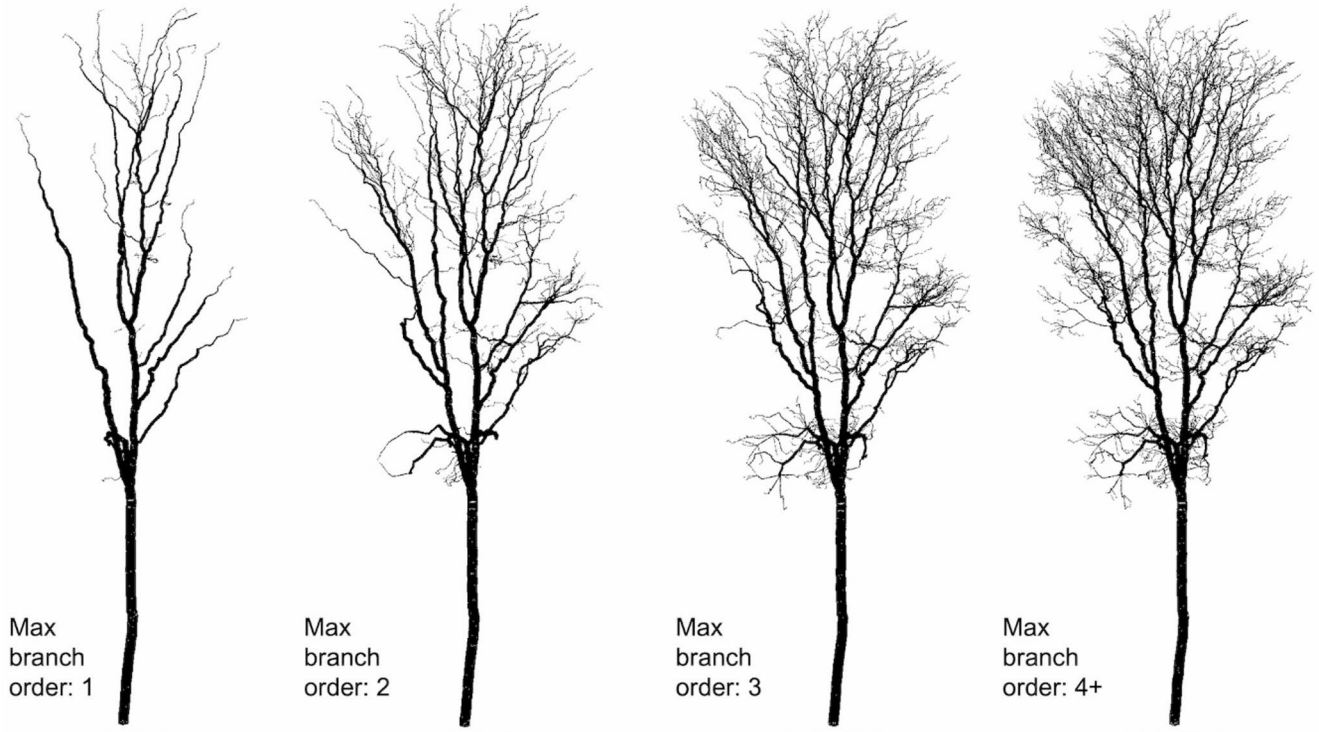

Fig. 1 An example of pruning. From left to right, the maximum number of branch orders is one, two, three, and four or more (no pruning). The 0th branch order is the main stem. The images are based on point clouds of a tree with a height of 27.35 m and a maximum branch order of seven

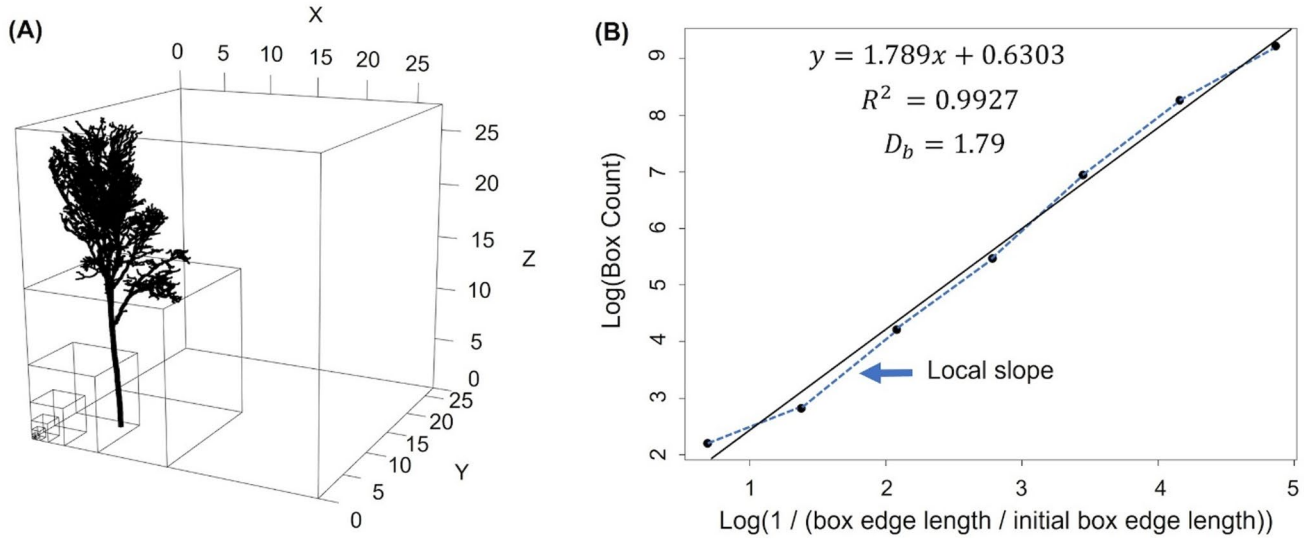

Fig. 2 Illustrations of the BCM. **(A)** Different box sizes with point clouds of a tree with a height of 27.35 m. **(B)** Derivation of D_b from a linear regression (solid line) and local slopes (dashed line). The illustrations were produced using the function *box_dimension* from the R package *rTwig* (Morales and MacFarlane 2024) and modified

lines and local slopes were also computed (Fig. 2B). Local slopes are defined as the slopes between neighboring data point pairs.

Placement effect

In practice, trees' positions and orientations in the coordinate system depend on the laser scanning campaign (e.g., position of terrestrial laser scanner, start position of mobile laser scanner) (Fig. 3). It is possible to understand these effects by changing the trees' positions by translation and their orientations by Z-axis rotation in the coordinate system. In this study, we assessed the effects of position and orientation separately. The initial box count is ignored in the D_b computation, and counting from the second box size affects the D_b. Therefore, we can examine the effect of position by translating trees from the reference within the second box side length in XYZ directions. Specifically, we first determined half the length of the initial box edge and created a sequence of 11equidistant points along that length. Then, using the first ten points, we created 1000 translation patterns (10(X)*10(Y)*10(Z) = 1000 translations for each non-pruned and pruned tree; 399,000 translations in total), including the reference position (i.e., no translation). In this way, we assumed that it is possible to assess the effect of position equally for trees of different sizes. To understand the effect of orientation, we rotated each tree at the reference around the Z-axis from 0° to 350° by 10° (i.e., 36 rotations for each non-pruned and pruned tree; 14,364 rotations in total). Lastly, the maximum difference of D_b (the difference between the maximum and minimum D_b values, hereafter denoted as $D_{b,\,diff}$) was calculated separately for translated and rotated point clouds. We decided on the procedures mentioned above due to their computational feasibility, and our investigations are by no means exhaustive. In this study, we investigated the potential effects of arbitrary tree placements related to laser scanning campaigns.

Statistical analysis

All statistical analyses were conducted in R version 4.4.2 (R Core Team 2024). To test the effect of branch reiteration on R^2 values, we fitted a linear mixed-effects model using the package *glmmTMB* (Brooks et al. 2017), with R^2 as the response and the maximum branch order (ranging from one to four or more) as the predictor. Tree ID (a unique identifier for each tree) was included as a random intercept. We chose the beta distribution as the response distribution family because R^2 values are bounded between 0 and 1.

By visually inspecting the distributions of D_b from translations and Z-rotations, we found that the ranges of D_b values were greatly larger for translations (Fig. 4). The ranges of D_b values from Z-rotations were around D_bs at the references and always within the ranges of D_b values from translations. The distribution of D_b from translations, in general, appeared unimodal and bell-shaped, with some differences in right- or left-skewness and spread. These observations suggest that the effect of positions strongly affects the D_b. Thus, to minimize the placement effect, we used the median R^2 values from translations for the model response. To visually inspect local slope patterns under different levels of branch reiteration for each tree, we visualized the median

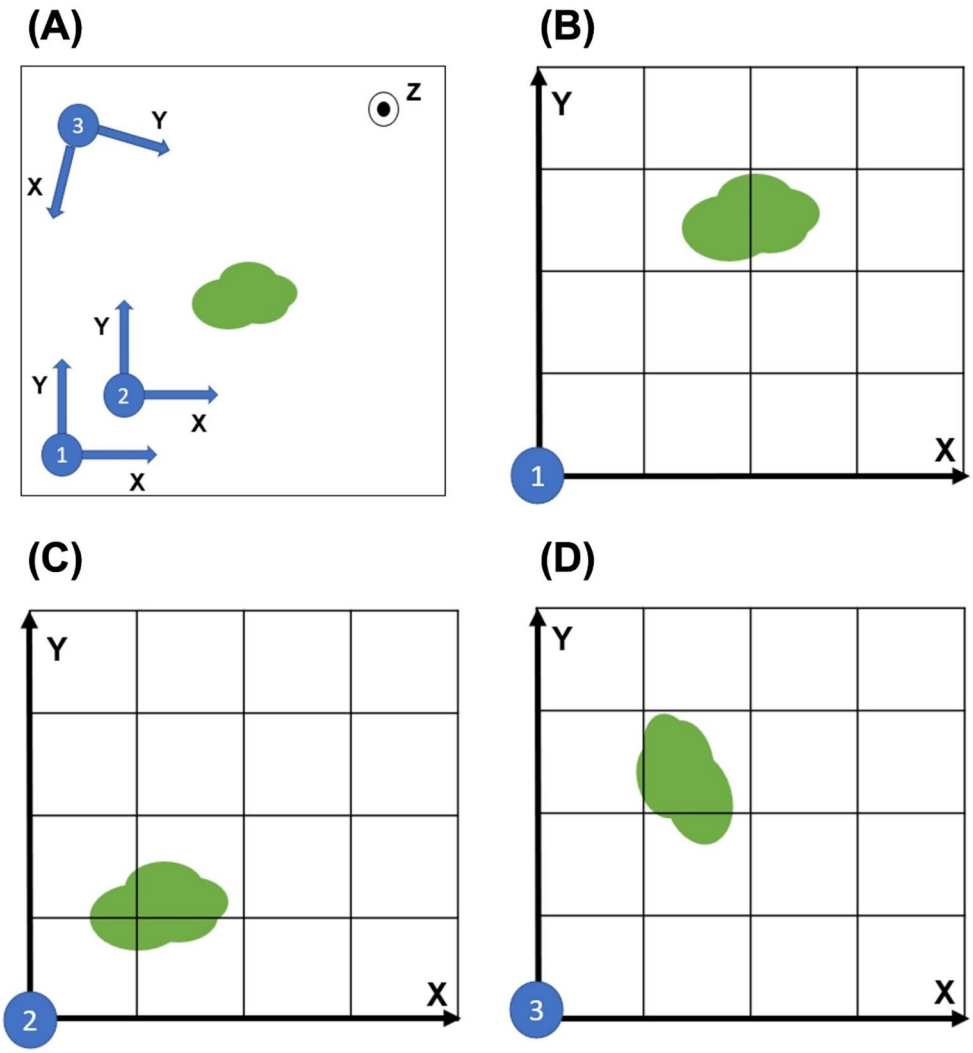

Fig. 3 Illustrations of the placement effect. (**A**) Numbers indicate the coordinate origins, and the arrows indicate the X and Y axes directions, depending on the specific laser scanning campaigns. A green object near the center is a tree's top canopy. Note that this is a top view, and the Z-axis coordinate origin can also differ. In (**B**), (**C**), & (**D**), the positions and/or the orientations of the tree differ in the coordinate systems according to (**A**). In (**B**) & (**C**), the positions are different. In (**D**), the position and orientation of the tree are different from those in (**B**) & (**C**)

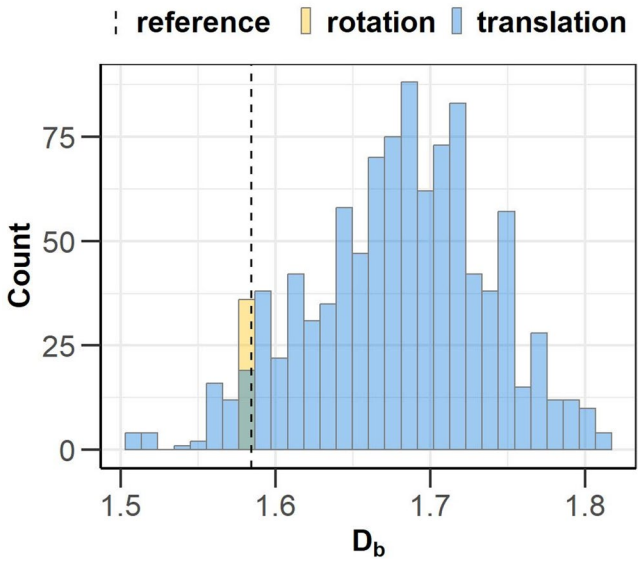

Fig. 4 An example of the D_b distribution. The blue and yellow shadings indicate translation and Z-rotation, respectively. The dashed line is the D_b value at the reference

and standard deviation (SD) of local slopes from translations against each interval of the scales. The median local slope was used to minimize the placement effect, and the SD of local slopes was used to show how local slope varies at each scale due to the placement effect.

We referred to Santon et al. (2023) for exploratory data analysis for the regression model. For model diagnostics, we used the packages *DHARMa* (Hartig 2024) (to assess model residuals using randomized quantile residuals) and *performance* (Lüdecke et al. 2021) (to assess the normality of random effects and perform a posterior predictive check). For model interpretation, we computed marginal and conditional R^2 values based on Nakagawa et al. (2017) using *performance* (Lüdecke et al. 2021). For data handling and visualization, we used the packages from *tidyverse* (Wickham et al. 2019) (e.g., *dplyr*, *tidyr*, *ggplot2*). Package dependencies for the R project used in this study were managed with the package *renv* (Ushey and Wickham 2024) for reproducibility. The R code and the lockfile containing

Table 1 Summary statistics of the maximum branch order, the D_b, and the $D_{b,\,diff}$

	Min.	1st Qu.	Median	Mean	3rd Qu.	Max.	SD
Max branch order	3.000	5.000	5.000	5.180	6.000	7.000	0.833
D_b (median)	1.331	1.606	1.689	1.674	1.765	1.872	0.113
$D_{b,\,diff}$ (translation)	0.183	0.285	0.337	0.341	0.379	0.523	0.066
$D_{b,\,diff}$ (Z-rotation)	0.004	0.011	0.017	0.022	0.026	0.090	0.016

D_b (median) is the median of D_b values calculated from translations to account for the placement effect

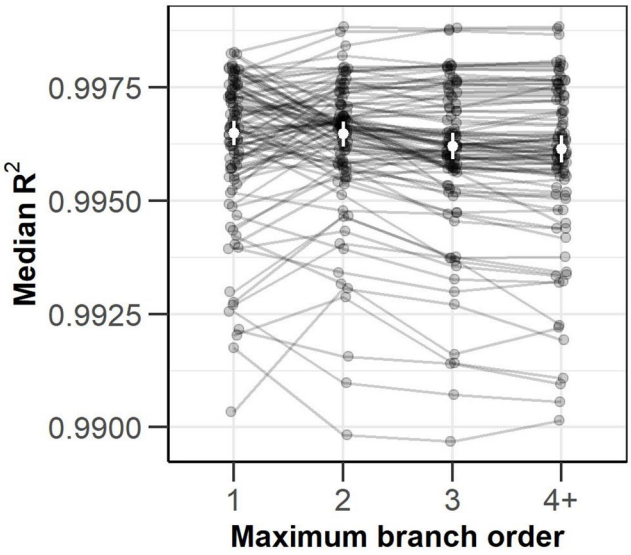

Fig. 5 Plot of median R^2 values against the maximum branch order. A maximum branch order of 4 + indicates four or more (no pruning). The white points indicate model-estimated means with the corresponding 95% confidence intervals above and below (conditional R^2: 1.000; marginal R^2: 0.014). The black points indicate observed values and are jittered for clarity. Points belonging to the same individuals are connected by lines. The median of R^2 values from translations was used to account for the placement effect

metadata about the packages used for this study are available in GRO.data at https://doi.org/10.25625/6IRTQM.

Results

In the dataset, the maximum branch order ranged from three to seven, with a mean of 5.180, and the D_b ranged from 1.331 to 1.872, with a mean of 1.674 (Table 1). The $D_{b,\,diff}$ from translations ranged from 0.183 to 0.523, and the mean was 0.341, while the $D_{b,\,diff}$ from Z-rotations was smaller. The range was 0.004–0.090, with a mean of 0.022 (Table 1). Comparing the $D_{b,\,diff}$ from translations and the $D_{b,\,diff}$ from Z-rotations of the same individuals, the $D_{b,\,diff}$ from Z-rotations was 93.4% lower on average.

Regardless of the maximum branch order, the model estimated means of R^2 values were over 0.995 (Fig. 5), and we did not observe an increasing trend in R^2 values as the maximum branch order increased, which is supported by the very low marginal R^2 (0.014) of the model. The observed minimum R^2 values were rounded to 0.990 for all the maximum branch orders.

Regardless of the maximum branch order, the local slope patterns in general showed an upward convex curve (Fig. 6A, C), which was less evident when the scale was limited due to the lower cutoff (Fig. 6E). Local slope values tended to be larger and more varied across scales as the maximum branch order increased (Fig. 6A, C), which was less evident when a tree's D_b was small (Fig. 6E). The local slope values among different maximum branch orders tended to converge at the beginning and the end of the scales (Fig. 6A, C, E). Regardless of the maximum branch order, the SD of the local slopes from translations at each interval of the scales, in general, showed an exponentially decreasing pattern as the scales became finer (Fig. 6B, D, F).

Discussion

We investigated the BCM's sensitivity to arbitrary tree placement in the coordinate system, as well as the BCM's R^2 values and local slope patterns under different levels of branch reiteration, using 100 European beech trees. Overall, we found that the D_b was sensitive to positions in the coordinate system ($D_{b,\,diff}$ (translation) ≥ 0.18) and less so to orientations ($D_{b,\,diff}$ (Z-rotation) ≤ 0.09). Also, we found that the R^2 values of the regression lines of the BCM were consistently high (≥ 0.990), regardless of the maximum branch order, even though the local slopes generally varied across scales with a systematic convex pattern.

BCM's sensitivity to arbitrary placement

Given that D_b values ranged from 1.33 to 1.87, even the low $D_{b,\,diff}$ values (0.2–0.3) from translations in the samples should be considered substantial (Table 1). On the other hand, $D_{b,\,diff}$ values from Z-rotations in the samples were considerably lower, with a maximum of 0.09 and a minimum of 0.004 (Table 1). The greater effect of position is likely because changing a tree's position in the coordinate system has a larger influence on the box counts at coarser scales than changing the orientation of the tree (Panico and Sterling 1995). The box count differences at coarser scales have a larger impact on local slopes compared to those at

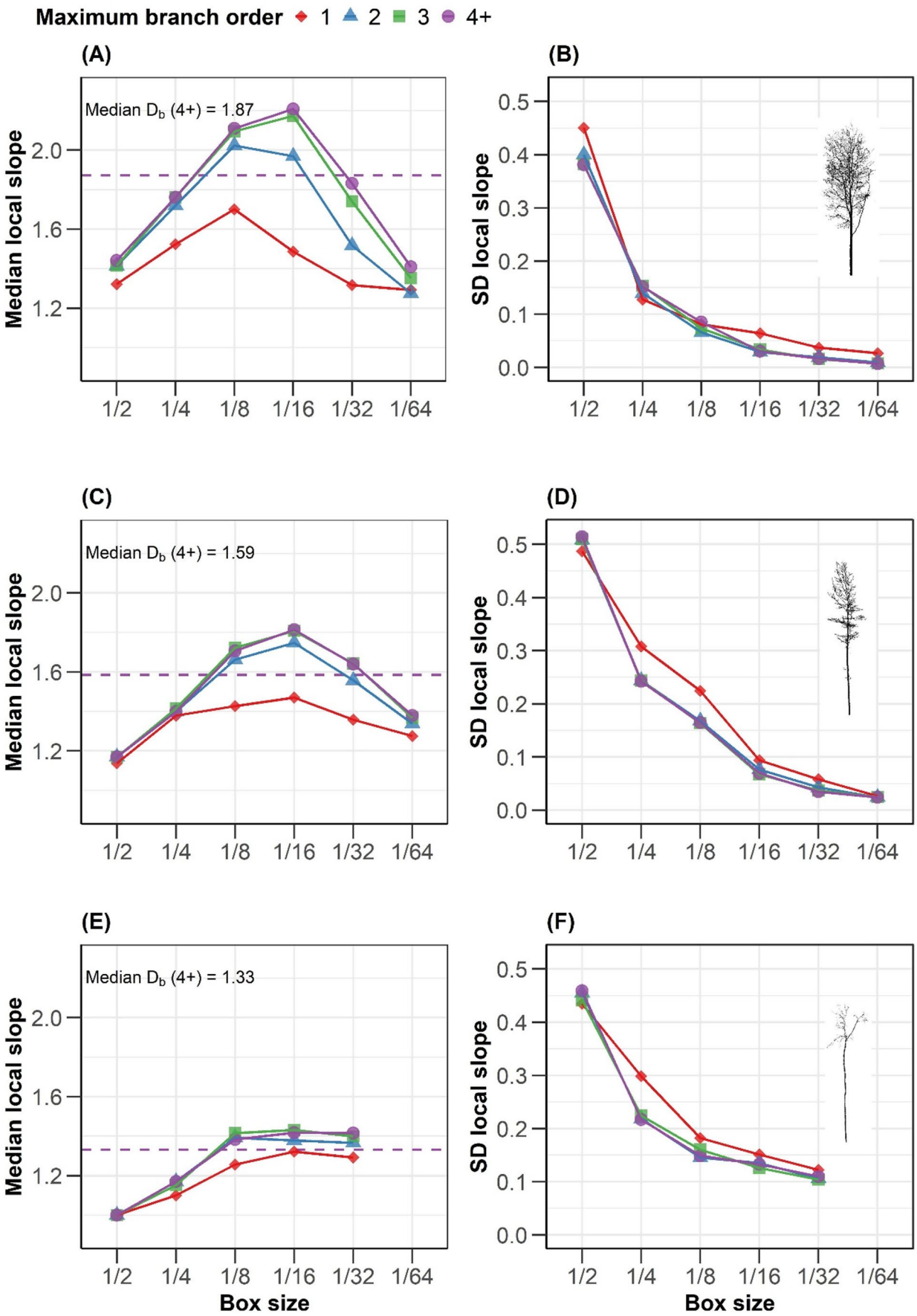
Maximum branch order 1 2 3 4+
(A)
Median D_b (4+) = 1.87
Median local slope
(B)
SD local slope
(C)
Median D_b (4+) = 1.59
Median local slope
(D)
SD local slope
(E)
Median D_b (4+) = 1.33
Median local slope
(F)
SD local slope
1/2 1/4 1/8 1/16 1/32 1/64
Box size

Fig. 6 Three examples of local slope patterns under different maximum branch orders. A maximum branch order of 4+indicates four or more (no pruning). **(A)**, **(C)**, **& (E)**: Median local slope from translations against box size (relative box edge length with respect to the initial box edge length). The box size is the starting point of the local slope. For example, the local slope value at a box size of 1/2 was calculated on the scale between 1/2 and 1/4. The dashed line is the median D_b from translations corresponding to the non-pruned trees (4+). **(B)**, **(D)**, **& (F)**: SD of local slopes from translations against box size. Note that there is no data point at a box size of 1/64 in **(E)** & **(F)** due to the lower cutoff of 20 cm. **(A)** & **(B)**: a tree with a median D_b of 1.87, a height of 27.99 m, and a maximum branch order of six; **(C)** & **(D)**: a tree with a median D_b of 1.59, a height of 26.53 m, and a maximum branch order of five; **(E)** & **(F)**: a tree with a median D_b of 1.33, a height of 18.33 m, and a maximum branch order of four; the corresponding images of the trees in **(B)**, **(D)**, **& (F)** are based on point clouds

finer scales due to the larger relative box count differences at coarser scales. For example, let's assume that due to the placement effect, at a coarse scale the box count increases from 10 to 12 (a 20% increase), and at a finer scale the box count increases from 1000 to 1020 (a 2% increase). When taking the logarithm of these values, the difference between log(10) and log(12) (ca. 0.18) is larger than the difference between log(1000) and log(1020) (ca. 0.020). This also explained why we observed larger SDs of local slope at coarser scales (Fig. 6B, D, F). These results suggest that when correlating the D_b with the tree's physical functions, the placement effect, especially due to position, reduces associations between the D_b and the tree's physical functions (Loke and Chisholm 2022), thereby reducing the predictive power of the D_b.

One quick fix for this issue is to standardize the trees' positions in the coordinate system, as we did when creating the reference (i.e., by setting the coordinate origin to the tree base). Although this does not address the placement effect due to orientation and the D_b value would be specific to how the positions of trees are standardized (Fig. 4), the $D_{b,\,diff}$ of our samples was reduced by 93.4%, on average. A more precise but computationally intensive approach to this issue is to find the minimum number of boxes necessary to cover a tree at each box size by implementing a pattern search algorithm, as in Bouda et al. (2016). Another simple way to address the issue is to remove the coarser scales from the D_b computation, as the largest variations in local slopes due to the placement effect occur at coarser scales (Fig. 6B, D, F) (Panico and Sterling 1995; Bouda et al. 2016). However, we already excluded the coarsest scale (i.e., the initial box) from the computation, and removing further scales will diminish the BCM's ability to capture the detailed distribution of tree structural elements in 3D space (Seidel 2018). Thus, applying an algorithm to find the minimum box counts at coarse scales could be another feasible remediation. Further research is needed to address the placement effect when using the BCM to measure tree structural complexity.

R^2 values and local slope patterns of the BCM

Trees tend to look self-similar and fractal due to their branch reiteration (Barthélémy and Caraglio 2007; Malhi et al. 2018). Thus, decreasing the branching repetition would reduce the self-similarity of trees, which should be reflected in the R^2 values of the BCM (Seidel 2018). Also, when R^2 values are high, we expect the objects to be self-similar, and local slope patterns tend to be more or less flat (Panico and Sterling 1995; Bouda et al. 2016). However, we found no practical differences in R^2 values among tree models with different maximum branch orders (Fig. 5). The R^2 values were consistently very high ($\geq$0.990). Moreover, by investigating local slope patterns, we found that, in general, the patterns were upward convex curves, and local slopes varied more across scales as the maximum branch order increased (Fig. 6A, C, E). These findings suggest that it is difficult to assume constant scaling properties (i.e., self-similarity) of the beech tree models based on the BCM, and the R^2 value of the BCM's regression is insensitive to local scaling pattern changes. Thus, the R^2 value is unlikely to be helpful for assessing self-similarity, as pointed out in some literature (e.g., Halley et al. 2004; Bouda et al. 2016).

The local slopes at the beginning of the scales seem to indicate the overall tree crown spread in space, which is likely determined by the first-order branches. This can be observed in the convergence of local slope values at the beginning of the scales among different maximum branch orders (Fig. 6A, C, E). On the other hand, the local slopes at the intermediate scales seem to indicate the density of branches present in the crown (Panico and Sterling 1995). This can be observed in the increased local slopes for higher maximum branch orders, which was less apparent when the D_b was smaller. Trees with a small D_b are structurally simple and have a pole-like structure (i.e., 1D) and created fewer variations in local slopes across scales (Fig. 6E). This does not mean they have reiterated architecture and are more fractal, but rather that they are close to 1D. The observed local slope convergence among different maximum branch orders at the end of the scale (Fig. 6A, C) seems to indicate that the box size was too small to observe any scaling differences. In other words, at this scale, boxes start to align with the tree, and the BCM does not meaningfully evaluate the distribution of tree elements in space. These observations suggest that investigating local slope patterns is more helpful for assessing the consistency of the scaling exponent of the BCM than relying on an R^2 value (Panico and Sterling 1995; Bouda et al. 2016; Cheeseman and Vrscay 2022). Also, the observed clear local scaling patterns suggest that the D_b is likely sensitive to the scales used for the computation, and standardizing scales may be necessary.

A tree crown is the result of genetics and environmental conditions; thus, the architecture of a tree growing in optimal conditions might correspond to the model of self-similarity. However, episodic stresses can alter the growth pattern of a tree, and damage can alter the already established architecture (Malhi et al. 2018). Our results indicate that the D_b of the sampled beech trees appears to depend on the scales used for computation, and it is hard to assume consistent scaling properties across scales. Thus, in the case of the sampled trees, referring the D_b to the fractal dimension is better to be avoided since there is not enough evidence from the BCM to claim self-similarity (Loke and Chisholm 2022). Based on our observations, the D_b of the sampled trees could instead be interpreted as a metric that quantifies the average spatial distribution and density of the tree's elements (i.e., stems, branches, twigs) (Panico and Sterling 1995; Cheeseman and Vrscay 2022), which still conforms with the intended use of the BCM to measure tree structural complexity (Seidel 2018). The strong relation between the D_b and important tree functions such as productivity and hydraulic processes proves that the D_b is a useful metric for tree structure-function research (e.g., Seidel et al. 2019a; Arseniou et al. 2021b; Saarinen et al. 2021; Dorji et al. 2021, 2024; Heidenreich and Seidel 2022). However, its interpretation in terms of tree structure should still be investigated, as our beech tree models are based on QSMs derived from point clouds obtained by mobile laser scanning and are not a perfect representation of the actual trees. We cannot exclude the possibility that our results contain methodological artifacts.

Conclusion

Using a wide range of European beech tree models derived from mobile laser scanning, the present study investigated the BCM's sensitivity to the arbitrary placement of a tree and R^2 values and local slope patterns of the BCM under different levels of branch reiteration. Our results indicate that the BCM is sensitive to the tree positions in the 3D coordinate system. Thus, the discovered placement effect, if not corrected for, reduces the robustness of D_b estimates for single trees. This could weaken the structure-function relationships under investigation, thereby reducing the D_b's predictive power. Thus, we suggest a simple remediation: standardizing the tree position with respect to the coordinate system, which reduced the variation in D_b values of the tree samples by an average of 93.4%. Our results also indicated that local slopes of the BCM varied across scales with a clear pattern, regardless of the maximum branch order, and R^2 values were insensitive to these local scaling pattern changes. Thus, it is recommended to use local slopes rather than R^2 to assess the consistent scaling properties of trees (i.e., self-similarity).

Acknowledgements We greatly acknowledge the freedom to conduct this research provided to us by the donation from 44moles GmbH, Göttingen.

Author contributions Conceptualization: TK, DS; Methodology: TK, DS, KK, AP; Formal analysis and investigation: TK; Writing – original draft: TK, KK; Writing – review and editing: TK, DS, KK, AP; Resources: AP, KK, DS; Supervision: DS. All authors read and approved the final manuscript.

Funding Open Access funding enabled and organized by Projekt DEAL. Funding was provided by the Deutsche Forschungsgemeinschaft (DFG, German Research Foundation) grant no. 316045089/GRK2300. TK was financially supported by the PhD scholarship provided by 44moles GmbH, Göttingen, during the preparation of this manuscript.

Data availability The datasets that support the current study's findings are available in GRO.data at https://doi.org/10.25625/6IRTQM.

Statements and Declarations

Competing Interests The authors have no relevant financial or non-financial interests to disclose.

References

Arseniou G, MacFarlane DW, Seidel D (2021a) Measuring the contribution of leaves to the structural complexity of urban tree crowns with terrestrial laser scanning. Remote Sens 13:2773. https://doi.org/10.3390/rs13142773

Arseniou G, MacFarlane DW, Seidel D (2021b) Woody surface area measurements with terrestrial laser scanning relate to the anatomical and structural complexity of urban trees. Remote Sens 13:3153. https://doi.org/10.3390/rs13163153

Barthélémy D, Caraglio Y (2007) Plant architecture: A dynamic, multilevel and comprehensive approach to plant form, structure and ontogeny. Ann Botany 99:375–407. https://doi.org/10.1093/aob/mcl260

Bouda M, Caplan JS, Saiers JE (2016) Box-counting dimension revisited: presenting an efficient method of minimizing quantization error and an assessment of the self-similarity of structural root systems. Front Plant Sci 7:149. https://doi.org/10.3389/fpls.2016.00149

Brooks ME, Kristensen K, van Benthem KJ et al (2017) GlmmTMB balances speed and flexibility among packages for zero-inflated generalized linear mixed modeling. R J 9:378–400. https://doi.org/10.32614/RJ-2017-066

Cazzolla Gatti R, Reich PB, Gamarra JGP et al (2022) The number of tree species on Earth. Proceedings of the National Academy of Sciences 119:e2115329119. https://doi.org/10.1073/pnas.2115329119

Cheeseman AK, Vrscay ER (2022) Estimating the fractal dimensions of vascular networks and other branching structures: some words of caution. Mathematics 10:839. https://doi.org/10.3390/math10050839

Da Silva D, Boudon F, Godin C et al (2006) A critical appraisal of the box counting method to assess the fractal dimension of tree crowns. In: Bebis G, Boyle R, Parvin B et al (eds) Advances in visual computing. Springer Berlin Heidelberg, Berlin, Heidelberg, pp 751–760

Dorji Y, Schuldt B, Neudam L et al (2021) Three-dimensional quantification of tree architecture from mobile laser scanning and geometry analysis. Trees 35:1385–1398. https://doi.org/10.1007/s00468-021-02124-9

Dorji Y, Isasa E, Pierick K et al (2024) Insights into the relationship between hydraulic safety, hydraulic efficiency and tree structural complexity from terrestrial laser scanning and fractal analysis. Trees 38:221–239. https://doi.org/10.1007/s00468-023-02479-1

Durrant TH, de Rigo D, Caudullo G (2016) *Fagus sylvatica* in europe: distribution, habitat, usage and threats. In: San-Miguel-Ayanz J, de Rigo D, Caudullo G et al (eds) European atlas of forest tree species. Publication Office of the European Union, Luxembourg, p e012b90

Falconer K (2003) Fractal geometry: mathematical foundations and applications, 2nd edn. Wiley, Chichester, UK

Falconer KJ (2013) Fractals: A very short introduction, 1st edn. Oxford University Press, Oxford

Guzmán QJA, Sharp I, Alencastro F, Sánchez-Azofeifa GA (2020) On the relationship of fractal geometry and tree–stand metrics on point clouds derived from terrestrial laser scanning. Methods Ecol Evol 11:1309–1318. https://doi.org/10.1111/2041-210X.13437

Hackenberg J, Morhart C, Sheppard J et al (2014) Highly accurate tree models derived from terrestrial laser scan data: A method description. Forests 5:1069–1105. https://doi.org/10.3390/f5051069

Hackenberg J, Spiecker H, Calders K et al (2015) SimpleTree —An efficient open source tool to build tree models from TLS clouds. Forests 6:4245–4294. https://doi.org/10.3390/f6114245

Halley JM, Hartley S, Kallimanis AS et al (2004) Uses and abuses of fractal methodology in ecology. Ecol Lett 7:254–271. https://doi.org/10.1111/j.1461-0248.2004.00568.x

Hartig F (2024) DHARMa: Residual diagnostics for hierarchical (multi-level / mixed) regression models. http://florianhartig.github.io/DHARMa/

Heidenreich MG, Seidel D (2022) Assessing forest vitality and forest structure using 3D data: A case study from the Hainich National Park, Germany. Front Forests Global Change 5:929106. https://doi.org/10.3389/ffgc.2022.929106

Laurans M, Munoz F, Charles-Dominique T et al (2024) Why incorporate plant architecture into trait-based ecology? Trends Ecol Evol 39:524–536. https://doi.org/10.1016/j.tree.2023.11.011

Loke LHL, Chisholm RA (2022) Measuring habitat complexity and Spatial heterogeneity in ecology. Ecol Lett 25:2269–2288. https://doi.org/10.1111/ele.14084

Lüdecke D, Ben-Shachar MS, Patil I et al (2021) Performance: an R package for assessment, comparison and testing of statistical models. J Open Source Softw 6:3139. https://doi.org/10.21105/joss.03139

Malhi Y, Jackson T, Patrick Bentley L et al (2018) New perspectives on the ecology of tree structure and tree communities through terrestrial laser scanning. Interface Focus 8:20170052. https://doi.org/10.1098/rsfs.2017.0052

Morales A, MacFarlane DW (2024) Reducing tree volume overestimation in quantitative structure models using modeled branch topology and direct twig measurements. Forestry: Int J for Res 98:394–409. https://doi.org/10.1093/forestry/cpae046

Nakagawa S, Johnson PCD, Schielzeth H (2017) The coefficient of determination R^2 and intra-class correlation coefficient from generalized linear mixed-effects models revisited and expanded. J R Soc Interface 14:20170213. https://doi.org/10.1098/rsif.2017.0213

Panico J, Sterling P (1995) Retinal neurons and vessels are not fractal but space-filling. J Comp Neurol 361:479–490. https://doi.org/10.1002/cne.903610311

Piboule A, Krebs M, Esclatine L, Hervé J-C (2013) Computree: A collaborative platform for use of terrestrial lidar in dendrometry: Presented at the International IUFRO Conference MeMoWood

R Core Team (2024) R: A Language and environment for statistical computing. R Foundation for Statistical Computing, Vienna, Austria

Reeve R (1992) A warning about standard errors when estimating the fractal dimension. Comput Geosci 18:89–91. https://doi.org/10.1016/0098-3004(92)90061-U

Saarinen N, Calders K, Kankare V et al (2021) Understanding 3D structural complexity of individual Scots pine trees with different management history. Ecol Evol 11:2561–2572. https://doi.org/10.1002/ece3.7216

Santon M, Korner-Nievergelt F, Michiels NK, Anthes N (2023) A versatile workflow for linear modelling in R. Front Ecol Evol 11:1065273. https://doi.org/10.3389/fevo.2023.1065273

Seidel D (2018) A holistic approach to determine tree structural complexity based on laser scanning data and fractal analysis. Ecol Evol 8:128–134. https://doi.org/10.1002/ece3.3661

Seidel D, Annighöfer P, Stiers M et al (2019a) How a measure of tree structural complexity relates to architectural benefit-to-cost ratio, light availability, and growth of trees. Ecol Evol 9:7134–7142. https://doi.org/10.1002/ece3.5281

Seidel D, Ehbrecht M, Dorji Y et al (2019b) Identifying architectural characteristics that determine tree structural complexity. Trees 33:911–919. https://doi.org/10.1007/s00468-019-01827-4

Ushey K, Wickham H (2024) renv: Project environments. https://CRAN.R-project.org/package=renv

Wickham H, Averick M, Bryan J et al (2019) Welcome to the tidyverse. J Open Source Softw 4:1686. https://doi.org/10.21105/joss.01686